Rend. Sem. Mat. Univ. Pol. Torino - Vol. 65, 2 (2007)
ISASUT Intensive Seminar

P. Cermelli - T. Armano*

FINE CROSS-SLIP OF A SCREW DISLOCATION IN ANTI-PLANE SHEAR

Abstract. In this work we present the main results of Armano and Cermelli [1] regarding the motion of a screw dislocation in a crystalline solid. It is well known that dislocations can only move along a finite number of crystallographic directions: in two dimensions, the resulting trajectories are piecewise rectilinear paths. However, in special situations such as near an attractor, dislocations are forced to move along curved paths: we characterize this class of motions as fine mixtures of crystallographic motions, using the notion of generalized curves due to L. C. Young, and explicitly compute the parametrized measure associated to a sequence of polygonals.

1. Introduction

We present here the results of Armano and Cermelli [1], and refer to that paper for the proofs of the main theorems and numerical simulations.

We study the motion of a rectilinear screw dislocation in a cylindrical crystalline elastic body, in the framework developed by Cermelli and Gurtin [2]. Peculiar to crystalline materials is the fact that dislocations are restricted to move along special planes, the so-called glide or slip planes.

In elastic materials, a state of stress induces a force on a dislocation, the so-called Peach-Köhler force (cf. [6], [3] and [2]), and the defect moves parallel to the direction on which the projection of this force is maximal (maximum dissipation criterion). Now, the motion of a straight dislocation can be described in terms of the intersection point of the dislocation line with an horizontal plane. The motion of the representative point can be viewed in turn as the solution of a plane dynamical system, obtained by projecting the Peach-Köhler force on the crystallographic directions. Since the number of such directions in a crystal is finite, it follows that the trajectories are piecewise rectilinear paths.

The general properties of this dynamical system have been studied in [2]: we focus here on a special situation, namely the motion near a curve S which is an attractor. The dislocation is attracted by S: when it reaches it, it cannot escape (since it would violate the maximum dissipation criterion), but it cannot move along S either, since it would, in general, violate the crystallographic restriction on the direction of motion. Hence, it seems natural to approximate the motion of the defect on S by a sequence of polygonals, which are piecewise parallel to the crystallographic directions but do not necessarily satisfy the maximum dissipation criterion at all times.

The main result of [1] is the proof that, if such a sequence is a maximizing

*This work was supported by the Italian M.U.R.S.T. research project "Modelli matematici per la scienza dei materiali" (Cofin 2002).

sequence for the dissipation, it converges to a unique smooth motion on S, which we refer to as *fine cross slip**.

To study the limits of maximizing sequences we use the notion of generalized curves due to L.C. Young, in their formulation known as parametrized (or Young) measures in the literature on the calculus of variations. Young measures provide a richer characterization of finely oscillating sequences than their weak limits: we compute the Young measure associated to sequences of polygonals maximizing the dissipation, and characterize fine cross slip as a fine mixture of crystallographic rectilinear motions, with weights depending on the direction of the attractor S.

2. Statement of the problem

We shortly summarize in this section the model discussed in [2]. Consider an elastic cylinder $B = \Omega \times \mathbb{R}$, with Ω a domain in $\mathbb{R}^2$. A *screw Volterra dislocation* is a singular displacement field on B which can be constructed by the following ideal procedure [8]: first cut the cylinder B along a vertical half-plane Π, then translate one of the faces along the cut by a constant vertical vector $\boldsymbol{b}$, glue back the faces along Π, and let the cylinder relax to an elastic equilibrium state (Figure 2). The resulting displacement field, measured with respect to the initial configuration, is smooth in $B \setminus \Pi$, but is discontinuous across Π with constant jump $\boldsymbol{b}$. The vertical line $\partial\Pi$ is called the *dislocation line*, and $\boldsymbol{b}$ is the *Burgers vector*. In order to avoid dealing with discontinuous displacement fields, it can be shown that a screw dislocation can be characterized equivalently in terms of a deformation field on $B \setminus \partial\Pi$, singular at $\partial\Pi$. In simple cases, the deformation field generated by a dislocation is independent of the vertical coordinate, and the problem admits a two-dimensional formulation in terms of planar fields on Ω, which are singular at $\boldsymbol{z} = \partial\Pi \cap \Omega$ (cf. [2]).

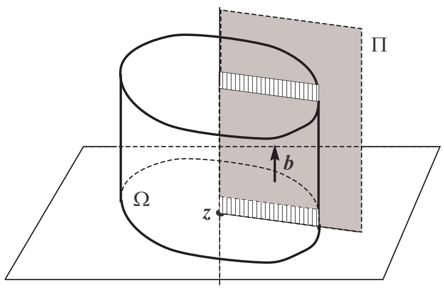

Figure 1: A screw Volterra dislocation in the cylinder $\Omega \times \mathbb{R}$.

Precisely, let Ω be a domain in $\mathbb{R}^2$, with cartesian coordinates (x, y) and associated basis $(\boldsymbol{e}_1, \boldsymbol{e}_2)$, and let $\boldsymbol{x}$ denote a generic point in Ω.

*Fine cross slip of screw dislocations has indeed been experimentally observed (cf., e.g., [5] and [4]).

Fix a defect position $\boldsymbol{z} \in \Omega$ and consider the solution $u : \Omega \to \mathbb{R}$ of the Neumann problem

$$\text{(1)} \qquad \begin{cases} \Delta u = 0 & \text{in } \Omega \\ \dfrac{\partial u}{\partial n} = -\boldsymbol{g}_0 \cdot \boldsymbol{n} + \sigma_0 & \text{on } \partial\Omega, \end{cases}$$

with Δ the Laplace operator, $\partial/\partial n$ the normal time-derivative on $\partial\Omega$, $\boldsymbol{n}$ the outward unit normal to $\partial\Omega$ and

$$\text{(2)} \qquad \boldsymbol{g}_0 = \boldsymbol{g}_0(\boldsymbol{x}, \boldsymbol{z}) = \frac{b}{2\pi|\boldsymbol{x} - \boldsymbol{z}|^2}\, \boldsymbol{e}_3 \times (\boldsymbol{x} - \boldsymbol{z}),$$

where b is a real constant, $\boldsymbol{e}_3 = \boldsymbol{e}_1 \times \boldsymbol{e}_2$ is a unit vector in $\mathbb{R}^3$ orthogonal to the plane containing Ω (so that $\boldsymbol{e}_3 \times (\cdot)$ represents a counterclockwise $\pi/2$-rotation in the Ω-plane), and $\sigma_0 = \sigma_0(\boldsymbol{x})$ is an assigned function on $\partial\Omega$. The field u represents the regular part of the displacement due to the dislocation at $\boldsymbol{z}$, while $\boldsymbol{g}_0$ is related to the singular part of the deformation.

For each fixed $\boldsymbol{z} \in \Omega$, the Neumann problem (1) has a unique smooth solution (modulo an additive constant), which we henceforth denote by

$$\text{(3)} \qquad u = u(\boldsymbol{x}, \boldsymbol{z}), \qquad \boldsymbol{x} \in \Omega.$$

Consider now the smooth vector field in Ω

$$\text{(4)} \qquad \boldsymbol{J}(\boldsymbol{x}) = b\, \nabla u(\boldsymbol{x}, \boldsymbol{x}) \times \boldsymbol{e}_3, \qquad \boldsymbol{x} \in \Omega,$$

where $\nabla u(\boldsymbol{x}, \boldsymbol{x}) = \nabla_{\boldsymbol{x}} u(\boldsymbol{x}, \boldsymbol{z})|_{\boldsymbol{z}=\boldsymbol{x}}$ is the gradient of the solution $u(\boldsymbol{x}, \boldsymbol{z})$ of (1), for a dislocation located at $\boldsymbol{z} = \boldsymbol{x}$. The vector field $\boldsymbol{J}(\boldsymbol{x})$ only depends on the domain Ω and the boundary conditions σ_0, and may be identified to the Peach-Köhler force on a dislocation located at $\boldsymbol{x} \in \Omega$.

Let now t denote time and $[0, T]$ be the time interval of interest. In order to study the behavior of a defect under the action of the force (4), consider a dislocation motion

$$\boldsymbol{z} : [0, T] \to \Omega.$$

Introducing the (finite) set of *crystallographic directions*

$$\mathcal{C} = \{\boldsymbol{s}_1, \ldots, \boldsymbol{s}_n\},$$

with $\boldsymbol{s}_i$ fixed unit vectors in $\mathbb{R}^2$, the basic physical idea is that a dislocation can only move parallel to a crystallographic direction $\boldsymbol{s} \in \mathcal{C}$ on which the projection of the force $\boldsymbol{J} \cdot \boldsymbol{s}$ is maximal, provided this is greater than a given threshold F, the so-called Peierls force (Figure 2). Therefore, we write the basic equation governing the motion of a dislocation as

$$\text{(5)} \qquad \dot{\boldsymbol{z}} = \boldsymbol{V}(\boldsymbol{z}), \qquad \boldsymbol{z} \in \Omega,$$

where the superposed dot denotes time-derivative, and where the vector field $\boldsymbol{V}$ is defined by

$$(6) \qquad \boldsymbol{V}(\boldsymbol{x}) := \begin{cases} \boldsymbol{0} & \text{if} \quad \boldsymbol{J}(\boldsymbol{x}) \cdot \boldsymbol{s} \leq F \quad \forall \boldsymbol{s} \in \mathcal{C}, \\ M\,(\boldsymbol{J}(\boldsymbol{x}) \cdot \boldsymbol{e}(\boldsymbol{x}) - F)\,\boldsymbol{e}(\boldsymbol{x}) & \text{otherwise,} \end{cases}$$

where $M > 0$ and $F \geq 0$ are given constants, and $\boldsymbol{e}(\boldsymbol{x}) \in \mathcal{C}$ is determined by the *maximum dissipation criterion*, i.e., the requirement that the projection of $\boldsymbol{J}(\boldsymbol{x})$ on $\boldsymbol{e}(\boldsymbol{x})$ be maximal, i.e.,

$$(7) \qquad \boldsymbol{J}(\boldsymbol{x}) \cdot \boldsymbol{e}(\boldsymbol{x}) = \max_{\boldsymbol{s} \in \mathcal{C},\ \boldsymbol{J} \cdot \boldsymbol{s} > F} \{\boldsymbol{J}(\boldsymbol{x}) \cdot \boldsymbol{s}\}.$$

It may happen that at some point $\boldsymbol{x}$ the maximization problem (7) admits two solutions: at such points the field $\boldsymbol{e}(\boldsymbol{x})$, and by consequence also $\boldsymbol{V}(\boldsymbol{x})$, is multi-valued. Indeed, $\boldsymbol{J} \cdot \boldsymbol{s}$ can have at most two maxima in $\mathcal{C}$ for $\boldsymbol{J}$ given. Assume in fact that there exist three distinct unit vectors $\boldsymbol{s}_1$, $\boldsymbol{s}_2$, $\boldsymbol{s}_3$ such that $\boldsymbol{J} \cdot \boldsymbol{s}_1 = \boldsymbol{J} \cdot \boldsymbol{s}_2 = \boldsymbol{J} \cdot \boldsymbol{s}_3$; then the endpoints of $\boldsymbol{s}_1$, $\boldsymbol{s}_2$ and $\boldsymbol{s}_3$ belong to the same straight line perpendicular to $\boldsymbol{J}$, which is impossible since the $\boldsymbol{s}_i$ are unit vectors.

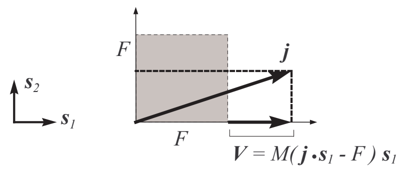

Figure 2: The definition of the vector field $\boldsymbol{V}$.

A detailed analysis of the phase portrait of the dynamical system (5) has been performed in [2], where it is shown that Ω splits into (i) regions where $\boldsymbol{V}(\boldsymbol{x}) = \boldsymbol{0}$, and the dislocation is stationary; (ii) *single slip regions* $R(\boldsymbol{s})$ (open regions in $\mathbb{R}^2$), in which $\boldsymbol{e}(\boldsymbol{x}) = \boldsymbol{s}$ is constant; and (iii) curves S on which $\boldsymbol{e}(\boldsymbol{x})$ is multi-valued. We are interested here in the motion on a so-called *attracting curve* (Figure 3).

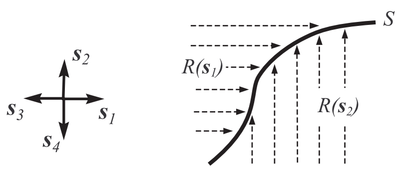

Figure 3: Attracting curve separating two single-slip regions

The motion of a dislocation, solution of (5), can be described as follows: consider, to fix ideas, a dislocation initially at $\boldsymbol{z}_0 \in R(\boldsymbol{s}_1)$: the evolution equation (5) reduces to

$$\dot{\boldsymbol{z}} = V_1(\boldsymbol{z})\boldsymbol{s}_1,$$

with $V_1(\boldsymbol{z}) = M(\boldsymbol{J}(\boldsymbol{z}) \cdot \boldsymbol{s}_1 - F)$. Hence, the dislocation moves along a straight line parallel to $\boldsymbol{s}_1$, until it reaches some point at the boundary of $R(\boldsymbol{s}_1)$. If this point belongs to an attractor, then the solution of (5) cannot be prolonged into the adjacent region, since it would violate the maximum dissipation criterion (Figure 3).

Hence, the problem seems to be ill-posed in the presence of an attractor. In order to remove the ambiguity, it was suggested in [2] that, when the dislocation reaches an attractor S, it continues to move along it according to an evolution equation of the form

$$\dot{\boldsymbol{z}} = \boldsymbol{w}(\boldsymbol{z}), \qquad \text{with} \quad \boldsymbol{w}(\boldsymbol{z}) = V_{12}(\boldsymbol{z})(\alpha_1(\boldsymbol{z})\boldsymbol{s}_1 + \alpha_2(\boldsymbol{z})\boldsymbol{s}_2), \tag{8}$$

where $V_{12}(\boldsymbol{z}) := \boldsymbol{J}(\boldsymbol{z}) \cdot \boldsymbol{s}_1 - F = \boldsymbol{J}(\boldsymbol{z}) \cdot \boldsymbol{s}_2 - F$, and α_1, α_2 are determined by solving

$$\begin{cases} \alpha_1 + \alpha_2 = 1, \\ \alpha_1(\boldsymbol{s}_1 - \boldsymbol{s}_2) \cdot (\nabla \boldsymbol{J})\boldsymbol{s}_1 + \alpha_2(\boldsymbol{s}_1 - \boldsymbol{s}_2) \cdot (\nabla \boldsymbol{J})\boldsymbol{s}_2 = 0. \end{cases} \tag{9}$$

The resulting smooth motion of the dislocation, referred to as *fine cross slip*, is therefore non-crystallographic, since it does not occur along a crystallographic direction $\boldsymbol{s} \in \mathcal{C}$. The purpose of the next section is to show that motion by fine cross slip (8) can be realized as the limit of a sequence of infinitesimal cross slips across the attracting curve S, when this sequence maximizes the dissipation.

Remark. Letting

$$\hat{V}(\boldsymbol{e}, \boldsymbol{J}) := \begin{cases} 0, & \text{if} \quad \boldsymbol{J} \cdot \boldsymbol{e} \leq F, \\ M(\boldsymbol{J} \cdot \boldsymbol{e} - F), & \text{if} \quad \boldsymbol{J} \cdot \boldsymbol{e} > F, \end{cases} \tag{10}$$

we may rewrite condition (7) as the requirement that motion may only occur in those directions $\boldsymbol{e}$ which maximize the *dissipation* $\hat{V}(\boldsymbol{s}, \boldsymbol{J})\boldsymbol{J} \cdot \boldsymbol{s}$, i.e.,

$$\hat{V}(\boldsymbol{e}, \boldsymbol{J})\, \boldsymbol{J} \cdot \boldsymbol{e} = \max_{s \in \mathcal{C}} \left[\hat{V}(\boldsymbol{s}, \boldsymbol{J})\, \boldsymbol{J} \cdot \boldsymbol{s} \right], \tag{11}$$

provided that $\hat{V}(\boldsymbol{e}, \boldsymbol{J}) > 0$. The equivalence of (7) and (11) follows from the fact that the function $M(\xi - F)\xi$ is monotonic with respect to ξ for $\xi > F$.

3. Convergence of sequences of admissible polygonals

We study here the motion of a dislocation near an attracting curve, in order to justify (8) rigorously. From now on we regard the vector field $\boldsymbol{J}(\boldsymbol{x})$ in (4) as assigned and smooth in Ω.

Let $\boldsymbol{z} : [0, T] \to \Omega$ be a given motion (not necessarily a solution of (5), (7), and (6)); writing

$$\dot{\boldsymbol{z}}(t) = V(t)\boldsymbol{e}(t), \qquad t \in [0, T], \tag{12}$$

with $V = |\dot{\boldsymbol{z}}|$ and $\boldsymbol{e} = \dot{\boldsymbol{z}}/|\dot{\boldsymbol{z}}|$, we say that $\boldsymbol{z}$ is *admissible* if

(i) $\boldsymbol{z}$ is continuous and piecewise smooth;

(ii) the direction of motion $\boldsymbol{e}(t)$ belongs to the set of crystallographic directions, and the velocity is a function of the projection of the force on that direction[†], i.e.,

$$\boldsymbol{e}(t) \in \mathcal{C} \quad \text{and} \quad V(t) = \hat{V}(\boldsymbol{e}(t), \boldsymbol{J}(\boldsymbol{z}(t))), \tag{13}$$

at each time t, with $\hat{V}$ given by (10).

An admissible motion does not necessarily satisfy the maximum dissipation criterion at all times, but its trajectory is a polygonal with edges parallel to the crystallographic directions.

We assume from now on that the set of crystallographic directions is

$$\mathcal{C} = \{\boldsymbol{s}_1, \boldsymbol{s}_2, -\boldsymbol{s}_1, -\boldsymbol{s}_2\}, \tag{14}$$

with $\boldsymbol{s}_1 = \boldsymbol{e}_1$ and $\boldsymbol{s}_2 = \boldsymbol{e}_2$, and consider two adjacent single slip regions $R(\boldsymbol{s}_1)$ and $R(\boldsymbol{s}_2)$, connected open sets in Ω such that[‡] $\overline{R(\boldsymbol{s}_1)} \cap \overline{R(\boldsymbol{s}_2)} \neq \emptyset$ and $\overline{R(\boldsymbol{s}_1)} \cap \partial\Omega = \emptyset$, $\overline{R(\boldsymbol{s}_2)} \cap \partial\Omega = \emptyset$. By definition, in $R(\boldsymbol{s}_1)$ and $R(\boldsymbol{s}_2)$ the dissipation is maximal in the directions $\boldsymbol{s}_1$ and $\boldsymbol{s}_2$ respectively, i.e.,

$$\begin{cases} \boldsymbol{x} \in R(\boldsymbol{s}_1) & \Rightarrow \quad \boldsymbol{s}_1 \cdot \boldsymbol{J}(\boldsymbol{x}) > \boldsymbol{s} \cdot \boldsymbol{J}(\boldsymbol{x}), \quad \forall \boldsymbol{s} \in \mathcal{C},\ \boldsymbol{s} \neq \boldsymbol{s}_1, \\ \boldsymbol{x} \in R(\boldsymbol{s}_2) & \Rightarrow \quad \boldsymbol{s}_2 \cdot \boldsymbol{J}(\boldsymbol{x}) > \boldsymbol{s} \cdot \boldsymbol{J}(\boldsymbol{x}), \quad \forall \boldsymbol{s} \in \mathcal{C},\ \boldsymbol{s} \neq \boldsymbol{s}_2. \end{cases} \tag{15}$$

Also, we assume that

$$\boldsymbol{J}(\boldsymbol{x})\cdot\boldsymbol{s}_1 > F \quad \text{and} \quad \boldsymbol{J}(\boldsymbol{x})\cdot\boldsymbol{s}_2 > F, \qquad \boldsymbol{x} \in \overline{R(\boldsymbol{s}_1)} \cup \overline{R(\boldsymbol{s}_2)}.$$

3.1. The definition of attracting curve

Let

$$G(\boldsymbol{x}) := (\boldsymbol{s}_2 - \boldsymbol{s}_1) \cdot \boldsymbol{J}(\boldsymbol{x}), \tag{16}$$

and assume that $\boldsymbol{J}$ is such that $\nabla G \neq 0$ in Ω. By definition,

$$G(\boldsymbol{x}) < 0 \quad \text{for} \quad \boldsymbol{x} \in R(\boldsymbol{s}_1) \qquad \text{and} \qquad G(\boldsymbol{x}) > 0 \quad \text{for} \quad \boldsymbol{x} \in R(\boldsymbol{s}_2),$$

so that, by the smoothness of G and the fact that $\nabla G \neq 0$, the set

$$S = \overline{R(\boldsymbol{s}_1)} \cap \overline{R(\boldsymbol{s}_2)},$$

is a smooth curve on which G vanishes, i.e.,

$$G(\boldsymbol{x}) = 0 \quad \Leftrightarrow \quad \boldsymbol{s}_1 \cdot \boldsymbol{J}(\boldsymbol{x}) = \boldsymbol{s}_2 \cdot \boldsymbol{J}(\boldsymbol{x}) \qquad \boldsymbol{x} \in S. \tag{17}$$

We say that S is an *attracting curve* for $R(\boldsymbol{s}_1)$ and $R(\boldsymbol{s}_2)$ if it satisfies the supplementary conditions

$$\boldsymbol{s}_1 \cdot \nabla G(\boldsymbol{x}) > 0, \qquad \boldsymbol{s}_2 \cdot \nabla G(\boldsymbol{x}) < 0, \qquad \boldsymbol{x} \in S. \tag{18}$$

[†]For $\boldsymbol{z}$ continuous and piecewise smooth, $\dot{\boldsymbol{z}}$ is the right time-derivative at corner points.
[‡]Here $\bar{R}$ denotes the closure of a set $R \subset \Omega$.

Hence, at an attracting curve, $\boldsymbol{s}_1$ points into $R(\boldsymbol{s}_2)$ and $\boldsymbol{s}_2$ points into $R(\boldsymbol{s}_1)$ (Figure 3(c)). We denote by

$$\boldsymbol{\tau} = \boldsymbol{e}_3 \times \frac{\nabla G}{|\nabla G|}$$

the tangent vector to S.

No admissible motion satisfying the maximum dissipation criterion can originate from an attracting curve S. To see this, consider an admissible motion along $\boldsymbol{s}_1$ with initial point on S: by $(18)_1$, G is increasing along $\boldsymbol{s}_1$, and the dislocation moves into the single slip region $R(\boldsymbol{s}_2)$. But in this region the dissipation is maximal in the direction $\boldsymbol{s}_2$, and the maximum dissipation criterion is violated.

Moreover, writing

$$\begin{cases} V_1(\boldsymbol{x}) := \hat{V}(\boldsymbol{s}_1, \boldsymbol{J}(\boldsymbol{x})) = M(\boldsymbol{s}_1 \cdot \boldsymbol{J}(\boldsymbol{x}) - F), \\ V_2(\boldsymbol{x}) := \hat{V}(\boldsymbol{s}_2, \boldsymbol{J}(\boldsymbol{x})) = M(\boldsymbol{s}_2 \cdot \boldsymbol{J}(\boldsymbol{x}) - F), \end{cases} \tag{19}$$

for the admissible velocities in the directions $\boldsymbol{s}_1$ and $\boldsymbol{s}_2$ at $\boldsymbol{x} \in \overline{R(\boldsymbol{s}_1)} \cup \overline{R(\boldsymbol{s}_2)}$, (17) implies that $V_1(\boldsymbol{x}) = V_2(\boldsymbol{x})$ at $\boldsymbol{x} \in S$, and we denote by

$$V(\boldsymbol{x}) := V_1(\boldsymbol{x}) = V_2(\boldsymbol{x}) \qquad \boldsymbol{x} \in S,$$

their common value. However, since at S the maximum dissipation criterion admits both $\boldsymbol{s}_1$ and $\boldsymbol{s}_2$ as solutions, the vector field $\boldsymbol{V}$ in (6) is multi-valued, with values

$$V(\boldsymbol{x})\boldsymbol{s}_1 \qquad \text{and} \qquad V(\boldsymbol{x})\boldsymbol{s}_2,$$

at $\boldsymbol{x} \in S$.

3.2. Admissible polygonals

We study here admissible motions which do not necessarily satisfy the maximum dissipation criterion. By definition, an admissible motion $\boldsymbol{z}$ is a time-parametrized polygonal with sides parallel to the crystallographic directions $\boldsymbol{s}_i \in \mathcal{C}$ and piecewise continuous speed given by (10). Restricting to admissible motions occurring in $\overline{R(\boldsymbol{s}_1)} \cup \overline{R(\boldsymbol{s}_2)}$ along the directions $\boldsymbol{s}_1$ and $\boldsymbol{s}_2$ only, we have

$$\text{either} \qquad \dot{\boldsymbol{z}}(t) = V_1(\boldsymbol{z}(t))\boldsymbol{s}_1 \qquad \text{or} \qquad \dot{\boldsymbol{z}}(t) = V_2(\boldsymbol{z}(t))\boldsymbol{s}_2,$$

for $t \in [0, T]$, where V_1 and V_2 are given by (19) and $\dot{\boldsymbol{z}}(t)$ is the right time-derivative at the corner points of the polygonal.

3.3. Sequences of admissible motions

The natural notion of convergence for sequences of admissible motions should account for the fact that the velocity oscillates between the directions $\boldsymbol{s}_1$ and $\boldsymbol{s}_2$, and therefore may only converge in average. Weak-$*$ convergence in $W^{1,\infty}((0, T), \mathbb{R}^2)$ serves the purpose. We say that a sequence of Lipschitz motions $\{\boldsymbol{z}_k\}$ converges weak-$*$ in $W^{1,\infty}((0,T),\mathbb{R}^2)$ if there exists a motion $\boldsymbol{\xi} \in W^{1,\infty}((0,T),\mathbb{R}^2)$ such that $\boldsymbol{z}_k \to \boldsymbol{\xi}$ strongly in $C([0,T],\mathbb{R}^2)$, and $\dot{\boldsymbol{z}}_k \overset{*}{\rightharpoonup} \dot{\boldsymbol{\xi}}$ in $L^\infty([0,T],\mathbb{R}^2)$, i.e.,

$$\sup_{t\in[0,T]} |\boldsymbol{z}_k(t) - \boldsymbol{\xi}(t)| \to 0,$$

and

$$\int_I (\dot{\boldsymbol{z}}_k(t) - \dot{\boldsymbol{\xi}}(t))\, dt \to 0,$$

for any interval $I \subset [0,T]$, provided $\{\dot{\boldsymbol{z}}_k(t)\}$ is bounded in $L^\infty([0,T],\mathbb{R}^2)$.

The weak limit of a sequence of admissible motions is characterized by the Young measure associated to the sequence of the velocities (cf. Young [9] or, for a more recent approach, [7]). Consider in fact a sequence $\{\boldsymbol{w}_k : (0,T) \to \mathbb{R}^2\}$ converging weak-$*$ to $\boldsymbol{w}_0$ in $L^\infty((0,T),\mathbb{R}^2)$. A Young measure associated with the sequence $\{\boldsymbol{w}_k\}$ is a family of probability measures $\{\nu_t\}_{t\in(0,T)}$ in $\mathbb{R}^2$ which depends measurably on t, i.e., for any $\varphi : \mathbb{R}^2 \to \mathbb{R}$ continuous, the function

$$\bar{\varphi}(t) = \int_{\mathbb{R}^2} \varphi(\boldsymbol{w})d\nu_t(\boldsymbol{w}) \tag{20}$$

is measurable. The fundamental property of ν_t is that, for any continuous φ, the sequence $\{\varphi(\boldsymbol{w}_k)\}$ converges (modulo a subsequence) weak-$*$ to $\bar{\varphi}$ in $L^\infty((0,T),\mathbb{R}^2)$, i.e.,

$$\int_I \varphi(\boldsymbol{w}_k(t))\, dt \to \int_I \int_{\mathbb{R}^2} \varphi(\boldsymbol{w})d\nu_t(\boldsymbol{w})\, dt, \tag{21}$$

for any interval $I \subset [0,T]$, provided that $\{\varphi(\boldsymbol{w}_k)\}$ is bounded in $L^\infty([0,T],\mathbb{R})$.

THEOREM 1. *Consider a sequence of admissible polygonals $\boldsymbol{z}_k(t)$ in the directions $\boldsymbol{s}_1$ and $\boldsymbol{s}_2$, converging weak-$*$ in $W^{1,\infty}((0,T),\mathbb{R}^2)$ as $k \to +\infty$ to a Lipschitz motion $\boldsymbol{\xi} \in W^{1,\infty}((0,T),\mathbb{R}^2)$. Then the Young measure associated to the sequence $\{\dot{\boldsymbol{z}}_k\}$ is*

$$\nu_t = \lambda_1(t)\, \delta_{V_1(\boldsymbol{\xi}(t))\boldsymbol{s}_1} + \lambda_2(t)\, \delta_{V_2(\boldsymbol{\xi}(t))\boldsymbol{s}_2}, \qquad t \in (0,T), \tag{22}$$

with $\delta_{V_1(\boldsymbol{\xi}(t))\boldsymbol{s}_1}$ and $\delta_{V_2(\boldsymbol{\xi}(t))\boldsymbol{s}_2}$ Dirac measures localized at $V_1(\boldsymbol{\xi}(t))\boldsymbol{s}_1$ and $V_2(\boldsymbol{\xi}(t))\boldsymbol{s}_2$ respectively, and

$$\lambda_1(t) = \frac{\dot{\boldsymbol{\xi}}(t)\cdot \boldsymbol{s}_1}{V_1(\boldsymbol{\xi}(t))}, \qquad \lambda_2(t) = \frac{\dot{\boldsymbol{\xi}}(t)\cdot \boldsymbol{s}_2}{V_2(\boldsymbol{\xi}(t))}. \tag{23}$$

Notice that, since the velocity of the limit motion is

$$\dot{\boldsymbol{\xi}}(t) = \lambda_1(t)V_1(\boldsymbol{\xi}(t))\boldsymbol{s}_1 + \lambda_2(t)V_2(\boldsymbol{\xi}(t))\boldsymbol{s}_2, \tag{24}$$

it follows that the weak limit of a sequence of admissible motions is not necessarily admissible, but can be represented as a fine mixture of crystallographic motions in the admissible directions $\boldsymbol{s}_1$ and $\boldsymbol{s}_2$.

COROLLARY 1. *Let S be an attracting curve separating two single slip regions $R(\boldsymbol{s}_1)$ and $R(\boldsymbol{s}_2)$: any sequence of admissible polygonals $\boldsymbol{z}_k(t)$ with directions $\boldsymbol{s}_1$ and $\boldsymbol{s}_2$ such that*

$$\operatorname{dist}(\boldsymbol{z}_k(t), S) \to 0, \tag{25}$$

uniformly in $t \in [0, T]$ as $k \to +\infty$, converges weak-$*$ in $W^{1,\infty}((0,T), \mathbb{R}^2)$ (and, in particular, uniformly) to a smooth motion $\boldsymbol{\xi}(t)$ on S with velocity

$$\dot{\boldsymbol{\xi}}(t) = \frac{V(\boldsymbol{\xi}(t))}{\boldsymbol{\tau}(\boldsymbol{\xi}(t)) \cdot (\boldsymbol{s}_1 + \boldsymbol{s}_2)}\, \boldsymbol{\tau}(\boldsymbol{\xi}(t)), \tag{26}$$

with $\boldsymbol{\tau}$ the unit tangent vector to S and $V(\boldsymbol{x}) := V_1(\boldsymbol{x}) = V_2(\boldsymbol{x})$ the speed evaluated at $\boldsymbol{x} \in S$ (cf. (19)). Moreover, the Young measure associated to the sequence $\{\dot{\boldsymbol{z}}_k\}$ is

$$\nu_t = \lambda_1(\boldsymbol{\xi}(t))\, \delta_{V(\boldsymbol{\xi}(t))\boldsymbol{s}_1} + \lambda_2(\boldsymbol{\xi}(t))\, \delta_{V(\boldsymbol{\xi}(t))\boldsymbol{s}_2}, \tag{27}$$

with

$$\lambda_1(\boldsymbol{x}) = \frac{\boldsymbol{\tau}(\boldsymbol{x}) \cdot \boldsymbol{s}_1}{\boldsymbol{\tau}(\boldsymbol{x}) \cdot (\boldsymbol{s}_1 + \boldsymbol{s}_2)}, \qquad \lambda_2(\boldsymbol{x}) = \frac{\boldsymbol{\tau}(\boldsymbol{x}) \cdot \boldsymbol{s}_2}{\boldsymbol{\tau}(\boldsymbol{x}) \cdot (\boldsymbol{s}_1 + \boldsymbol{s}_2)}, \tag{28}$$

for a.e. $\boldsymbol{x} \in S$.

Notice that, even though each admissible motion $\boldsymbol{z}_k(t)$ does not necessarily satisfy the maximum dissipation criterion for all $t \in [0, T]$, the sequence $\boldsymbol{z}_k$ is a maximizing sequence for the dissipation, since the limit motion $\boldsymbol{\xi}$ satisfies the maximum dissipation criterion (recall, though, that the limit motion is not admissible). To see this, let $J(\boldsymbol{x}) := \boldsymbol{J}(\boldsymbol{x}) \cdot \boldsymbol{s}_1 = \boldsymbol{J}(\boldsymbol{x}) \cdot \boldsymbol{s}_2$ and $V(\boldsymbol{x}) := V_1(\boldsymbol{x}) = V_2(\boldsymbol{x})$ for $\boldsymbol{x} \in S$ (cf. (17)): the maximum dissipation (among all admissible motions) at $\boldsymbol{x} \in S$ is (cf. (11) and (15))

$$\max_{\boldsymbol{s} \in \mathcal{C}} \{\hat{V}(\boldsymbol{s}, \boldsymbol{J}(\boldsymbol{x}))\, \boldsymbol{J}(\boldsymbol{x}) \cdot \boldsymbol{s}\} = J(\boldsymbol{x})V(\boldsymbol{x}), \tag{29}$$

while the dissipation relative to the limit motion $\boldsymbol{\xi}(t)$ is

$$\boldsymbol{J}(\boldsymbol{\xi}(t)) \cdot \dot{\boldsymbol{\xi}}(t) = \frac{V(\boldsymbol{\xi}(t))}{\boldsymbol{\tau}(\boldsymbol{\xi}(t)) \cdot (\boldsymbol{s}_1 + \boldsymbol{s}_2)}\, \boldsymbol{J}(\boldsymbol{\xi}(t)) \cdot \boldsymbol{\tau}(\boldsymbol{\xi}(t)) = V(\boldsymbol{\xi}(t)) J(\boldsymbol{\xi}(t)), \tag{30}$$

since $\boldsymbol{J} = J(\boldsymbol{s}_1 + \boldsymbol{s}_2)$, and these expressions coincide at $\boldsymbol{x} = \boldsymbol{\xi}(t)$.

Also, it is not difficult to prove that (26) coincides with (8). In fact, solving system $(8)_2$ and recalling (16), we obtain

$$\begin{cases} \alpha_1 = \dfrac{(\boldsymbol{s}_2 - \boldsymbol{s}_1) \cdot (\nabla \boldsymbol{J})\boldsymbol{s}_2}{(\boldsymbol{s}_2 - \boldsymbol{s}_1) \cdot (\nabla \boldsymbol{J})\boldsymbol{s}_2 - (\boldsymbol{s}_2 - \boldsymbol{s}_1) \cdot (\nabla \boldsymbol{J})\boldsymbol{s}_1} = \dfrac{\nabla G \cdot \boldsymbol{s}_2}{\nabla G \cdot \boldsymbol{s}_2 - \nabla G \cdot \boldsymbol{s}_1}, \\ \alpha_2 = \dfrac{-(\boldsymbol{s}_2 - \boldsymbol{s}_1) \cdot (\nabla \boldsymbol{J})\boldsymbol{s}_1}{(\boldsymbol{s}_2 - \boldsymbol{s}_1) \cdot (\nabla \boldsymbol{J})\boldsymbol{s}_2 - (\boldsymbol{s}_2 - \boldsymbol{s}_1) \cdot (\nabla \boldsymbol{J})\boldsymbol{s}_1} = -\dfrac{\nabla G \cdot \boldsymbol{s}_1}{\nabla G \cdot \boldsymbol{s}_2 - \nabla G \cdot \boldsymbol{s}_1}, \end{cases}$$

with G given by (16). Now, noting that $\nabla G \cdot \boldsymbol{s}_2 = \nabla G \cdot \boldsymbol{e}_3 \times \boldsymbol{s}_1 = -\boldsymbol{e}_3 \times \nabla G \cdot \boldsymbol{s}_1 = -|\nabla G|\boldsymbol{\tau} \cdot \boldsymbol{s}_1$, and $\nabla G \cdot \boldsymbol{s}_1 = -\nabla G \cdot \boldsymbol{e}_3 \times \boldsymbol{s}_2 = \boldsymbol{e}_3 \times \nabla G \cdot \boldsymbol{s}_2 = |\nabla G|\boldsymbol{\tau} \cdot \boldsymbol{s}_2$, we find

$$\alpha_1 = \frac{\boldsymbol{\tau} \cdot \boldsymbol{s}_1}{\boldsymbol{\tau} \cdot \boldsymbol{s}_1 + \boldsymbol{\tau} \cdot \boldsymbol{s}_2}, \qquad \alpha_2 = \frac{\boldsymbol{\tau} \cdot \boldsymbol{s}_2}{\boldsymbol{\tau} \cdot \boldsymbol{s}_1 + \boldsymbol{\tau} \cdot \boldsymbol{s}_2},$$

which yields (26) recalling that V_{12} coincides with V in our present notation.

3.4. Sequences of admissible polygonals maximizing the dissipation

In this section we show that every sequence of polygonals maximizing the dissipation converges to the smooth motion $\boldsymbol{\xi}$ on S given by (26).

For $\boldsymbol{x} \in \Omega$, let $V_M(\boldsymbol{x})$ and $\boldsymbol{e}_M(\boldsymbol{x})$ denote the speed and direction of motion selected by the maximum dissipation criterion (11) among all admissible velocity fields, i.e. such that

$$V_M(\boldsymbol{x})\boldsymbol{e}_M(\boldsymbol{x}) \cdot \boldsymbol{J}(\boldsymbol{x}) = \max_{\boldsymbol{s} \in \mathcal{C}} \left\{ \hat{V}(\boldsymbol{s}, \boldsymbol{J}(\boldsymbol{x}))\, \boldsymbol{s} \cdot \boldsymbol{J}(\boldsymbol{x}) \right\}, \tag{31}$$

where $\hat{V}$ is given by (10). Notice that, even though $\boldsymbol{e}_M(\boldsymbol{x})$ is in general multi-valued at S, the maximum dissipation (31) is single valued everywhere. Consider the function $D : \Omega \times \mathbb{R}^2 \to \mathbb{R}$ defined by

$$D(\boldsymbol{x}, \boldsymbol{w}) = \boldsymbol{J}(\boldsymbol{x}) \cdot (V_M(\boldsymbol{x})\boldsymbol{e}_M(\boldsymbol{x}) - \boldsymbol{w})\,. \tag{32}$$

For a given motion $\boldsymbol{z} \in W^{1,\infty}((0,T), \mathbb{R}^2)$ the real function $D(\boldsymbol{z}(t), \dot{\boldsymbol{z}}(t))$ belongs to $L^\infty((0,T), \mathbb{R})$, and measures the difference between the maximum possible dissipation and the actual dissipation at each time.

Fix $\boldsymbol{z}_0 \in S$ and consider the set of admissible curves originating from $\boldsymbol{z}_0$:

$$\begin{aligned} \mathcal{A} \;=\; & \Big\{ \boldsymbol{z} : [0,T] \to \mathbb{R}^2 \;:\; \boldsymbol{z} \text{ piecewise smooth},\; \boldsymbol{z}(0) = \boldsymbol{z}_0 \in S \text{ and} \\ & \text{either} \quad \dot{\boldsymbol{z}}(t) = V_1(\boldsymbol{z}(t))\boldsymbol{s}_1 \quad \text{or} \quad \dot{\boldsymbol{z}}(t) = V_2(\boldsymbol{z}(t))\boldsymbol{s}_2,\; t \in [0,T] \Big\}, \end{aligned}$$

where $\dot{\boldsymbol{z}}$ denotes the right time-derivative at corner points of the polygonals.

By definition

$$D(\boldsymbol{z}(t), \dot{\boldsymbol{z}}(t)) \geq 0, \qquad \forall \boldsymbol{z} \in \mathcal{A}, \forall t \in [0,T], \tag{33}$$

although D can be negative for some non admissible motion.

Consider now the functional associated to D,

$$E(\boldsymbol{z}) = \int_0^T D(\boldsymbol{z}(t), \dot{\boldsymbol{z}}(t))\, dt = \int_0^T \boldsymbol{J}(\boldsymbol{z}(t)) \cdot (V_M(\boldsymbol{z}(t))\boldsymbol{e}_M(\boldsymbol{z}(t)) - \dot{\boldsymbol{z}}(t))\; dt, \tag{34}$$

defined for $\mathbf{z} \in W^{1,\infty}((0,T),\mathbb{R}^2)$. By the discussion following (18), no admissible motion satisfying the maximum dissipation criterion can originate from S, so that E is strictly positive on $\mathcal{A}$. Indeed, as we shall show in the next section,

$$\inf_{\mathbf{z}\in\mathcal{A}} E(\mathbf{z}) = 0, \tag{35}$$

and the infimum is not attained on $\mathcal{A}$.

THEOREM 2. *Any sequence of admissible polygonals $\{\mathbf{z}_k\} \subset \mathcal{A}$ minimizing E (or, equivalently, maximizing the dissipation), i.e., such that*

$$\lim_{k\to+\infty} E(\mathbf{z}_k) = 0, \tag{36}$$

converges weak-$*$ in $W^{1,\infty}((0,T),\mathbb{R}^2)$ to the smooth motion $\boldsymbol{\xi}(t)$ on S, whose velocity is (26).

Theorem 2 is the main result of this paper.

References

[1] ARMANO T. AND CERMELLI P., *Non-crystallographic motion of a dislocation as a fine mixture of rectilinear paths*, SIAM J. Applied Mathematics **64** (2004), 2121–2143.

[2] CERMELLI P. AND GURTIN M.E., *The motion of screw dislocations in materials undergoing anti-plane shear: glide, cross-slip, fine cross-slip*, Arch. Rational Mech. Anal., **148** (1) (1999), 3–52.

[3] ESHELBY J.D., *Energy relations and the energy-momentum tensor in continuum mechanics*, in: "Inelastic behavior of solids" (Eds. Kanninen M., Adler W., Rosenfield A. and Jaffee R.), McGraw-Hill, New York 1970, 77–115.

[4] HIRTH J.P. AND LOTHE J., *Theory of dislocations*, McGraw-Hill, New York 1982.

[5] KUHLMANN-WILSDORF D., *Theory of plastic deformation: properties of low energy dislocation structures*, Mater. Sci. Eng. A **113** (1989), 1–41.

[6] PEACH M. AND KÖHLER J.S., *The forces exerted on dislocations and the stress fields produced by them*, Phys. Rev. **80** (3) (1950), 436–439.

[7] PEDREGAL P., *Parametrized measures and variational principles*, Birkhäuser, Basel 1997.

[8] VOLTERRA V., *Sur l'équilibre del corps élastiques multiplement connexes*, Ann. Ec. Norm. **24** (1907), 401–451.

[9] YOUNG L.C., *Lectures on the calculus of variations and optimal control theory*, Saunders, Philadelphia 1969.

AMS Subject Classification: 74B99, 74H15, 65P99, 74E15.

Paolo CERMELLI and Tiziana ARMANO, Department of Mathematics, University of Turin, Via Carlo Alberto 10, 10123, Turin, ITALY
e-mail: `paolo.cermelli@unito.it, tiziana.armano@unito.it`